Strathprints Institutional Repository

A Family of Nitrogen-Enriched Metal Organic Frameworks with CCS Potential

Emma Dooris [1,2]**, Craig A. McAnally** [1,2]**, Edmund J. Cussen** [1]**, Alan R. Kennedy** [1] **and Ashleigh J. Fletcher** [1,2,*]

[1] Department of Pure and Applied Chemistry, University of Strathclyde, Glasgow G1 1XL, UK;
dooris.e@pg.com (E.D.); craig.mcanally@strath.ac.uk (C.A.M.); edmund.cussen@strath.ac.uk (E.J.C.);
a.r.kennedy@strath.ac.uk (A.R.K.)

[2] Chemical and Process Engineering, University of Strathclyde, Glasgow G1 1XJ, UK

[*] Correspondence: ashleigh.fletcher@strath.ac.uk; Tel.: +44-141-548-2431

Abstract: Materials with enhanced carbon capture capacities are required to advance post-combustive amelioration methods; these are necessary to reduce atmospheric carbon dioxide emissions and the associated rate of global temperature increase. Current technologies tend to be very energy intensive processes with high levels of waste produced; this work presents three new metal organic framework materials with embedded Lewis base functionalities, imparted by the nitrogen-rich ligand, demonstrating an affinity for carbon dioxide. Thus, we report the synthesis and characterization of a series of metal organic framework materials using a range of metal centers (Co, Ni, and Zn) with the 1,4-bis(pyridin-4-yl)-1,2,4,5-tetrazine organic linker, in the presence of ammonium hexafluorosilicate. Three distinct crystal structures are reported for Zn-pytz(hydro) 1D chains, and Ni-pytz and Co-pytz isostructural 1D Ladders. Co-pytz shows an uptake of 47.53 mg CO_2/g of sorbent, which equates to 15 wt % based on available nitrogen sites within the structure, demonstrating potential for carbon capture applications.

1. Introduction

Metal-organic frameworks (MOFs), synthesized using metal containing nodes and multidentate organic linkers, are one family of porous materials that have attracted significant interest for use in a range of sectors due to their inherent properties, including large surface areas and uniform porosities, which can be functionalized to suit specific applications. As a result, myriad MOFs have been synthesized [1] and characterized with respect to applications in adsorption [2,3], catalysis [4,5], sensing [6–8], gas storage [2,9,10] and separation [3,11]. The field of carbon capture is a key potential area for development of nanoporous materials, including MOFs [3], which present new structural effects, including the selective diffusion of guest species [11,12], that can be exploited to enhance adsorption and/or retention of gases. Increasing greenhouse gas emissions, of which carbon dioxide (CO_2) is a major constituent, have contributed to global climatic changes, hence, amelioration methods are essential [13] to stem the rise and, possibly, reverse current upward trends. Anthropogenic energy consumption currently requires the use of fossil fuel powered electricity plants. Such point sources, with carbon capture capabilities, utilize the most technologically feasible methods of carbon capture at this time [3], including absorption of CO_2 gas in aqueous alkanolamine solutions to afford separation [14]; however, such methods suffer a number of problems, comprising significant energy penalties for alkanolamine recovery (related to the high heat capacity of water), solvent degradation and associated waste products, as well as contaminant issues. As an alternative, the use of solid MOF adsorption beds

can offer reduced processing issues, such as increased thermal stability [3], as well as a reduction in energy demand, as many MOFs exhibit lower heat capacities and offer physical or pseudo-physical sorption compared to the chemical reactions observed for amines. The application of MOFs in gas sensing and membrane-based separation processes is a growth area [15–18], benefitting from the mild synthesis conditions, modular constructive approaches, tunability of porosity and functionalization of MOFs, which have also shown high chemical and thermal stability [19–21], and recent work has looked to apply MOFs to CO_2 adsorption to ameliorate the effects of energy related emissions [22,23]. These studies have focused on modifying either the secondary building units (SBUs) or multidentate organic ligands to enhance CO_2 adsorption; exploitation of unsaturated metal centers (UMCs) of SBUs [24,25] obtained via removal of terminal ligands invokes interactions between the UMCs and the highly polarizable quadrupole moment of CO_2. Alternatively, researchers have decorated the directing ligands using nitrogen containing groups, e.g., azo, triazole, tetrazole, acylamide, which are subsequently incorporated into the MOF structure; these nitrogen rich groups act as Lewis base sites, whereby their localized dipoles induce dispersive and electrostatic forces in the quadrupole moment of the Lewis acid CO_2, and the resulting MOFs exhibit enhanced CO_2 adsorption uptakes [26–29]. Consequently, we have synthesized and characterized a family of MOFs using the nitrogen containing ligand 1,4-bis(pyridin-4-yl)-1,2,4,5-tetrazine (pytz), with SBUs based on transition metal elements with the aim to reduce overall costs of manufacture and create a more sustainable MOF system. Herein, we report three new synthesized crystal structures $[Zn(pytz(hydrolyzed))_2(OH_2)_2(OCOCH_3)_2] \cdot H_2O$, $[Ni(pytz)_{1.5}(NO_3)_2] \cdot n$DCM ($n$ = 2–3) and $[Co_2(pytz)_3(NO_3)_4] \cdot n$DCM ($n$ = 4–6). The CO_2 adsorption behavior of $[Co_2(pytz)_3(NO_3)_4] \cdot n$DCM ($n$ = 4–6) is also presented.

2. Experimental

2.1. Materials Used

Nickel nitrate hexahydrate (98%), cobalt nitrate hexahydrate (98%–102%), zinc nitrate hexahydrate (98%), ethanol (⩾99.8%), dichloromethane (>99%), dimethylformamide (99.8%) were purchased from Sigma Aldrich (Poole, UK), ammonium hexafluorosilicate (98%) was purchased from Alfa Aesar (Heysham, UK). 1,4-bis(pyridin-4-yl)-1,2,4,5-tetrazine (pytz) (>98%) was purchased from TCI UK (Oxford, UK), and all chemicals were used as received.

2.2. Methods

2.2.1. Single Crystal Synthesis

Two methods were used to obtain single crystals for Single Crystal X-ray Diffraction (SCXRD). The layering method used to synthesize single crystals of Ni-pytz and Co-pytz was based on the work of Bisht & Suresh [30]. The order of the layers is dependent on the density of the solvents in which the precursors are dissolved, 3–4 mL of the "bottom" layer was carefully pipetted into the vial, a 1 mL buffer layer was added, before 3–4 mL of the "top" linker solution was layered on top. The sealed vessels were left undisturbed, under ambient conditions, for 3 weeks. Single crystals of Ni-pytz and Co-pytz were obtained by layering a 10 mL vial with the following composition: either 0.05 mmol $Ni(NO_3)_2 \cdot 6H_2O$ or 0.1 mmol $Co(NO_3)_2 \cdot 6H_2O$, and 0.08 mmol $(NH_4)_2SiF_6$ in 10 mL of ethanol as the top (4 mL) layer, and 0.1 mmol pytz in 10 mL dichloromethane as the bottom (4 mL) layer. Solids were harvested after 3 weeks. Crystals obtained from this solvent matrix cell lose their crystallinity on removal of the mother-liquor, indicated by the fact that they cease to show extinction under polarized light. Single crystals of Zn-pytz(hydro), were produced by autoclave synthesis, the procedure used was adapted from those of Hijikata *et al.* [31] and Hulvey *et al.* [32]. 0.3 mmol $Zn(NO_3)_2 \cdot 6H_2O$, 0.9 mmol $(NH_4)_2SiF_6$ and 0.6 mmol pytz in a 15 mL of 1 part dimethylformamide to 4 parts H_2O was heated at 383 K for 18 h, before cooling to 293 K at 5 K/min. Crystallization was further promoted by inclusion of previously prepared Zn-pytz(hydro) crystalline material.

2.2.2. Single Crystal X-ray Diffraction (SCXRD)

Crystallographic measurements were conducted at 123 K using an Oxford Diffraction diffractometer equipped with a CCD detector (Rigaku, Oxford, UK). All structures were refined against F^2 to convergence using all unique reflections and the program Shelxl [33]. The SQUEEZE routine within PLATON was applied to remove any disordered solvent molecules from crystallographic voids to reduce distortion in the crystal structure. Void calculations were performed using Oscail (National University of Ireland, Galway, Ireland) and Diamond (Crystal Impact, Bonn, Germany) software packages , void sizes were based on the radius of a CO_2 molecule (1.76 Å), determined from the assumption that CO_2 molecules can rotate about a perfect sphere of radius equivalent to the combined length of a C=O bond (1.163 Å [34]) and the radius of an O atom (0.60 Å [34]), and solvent molecules within voids would be completely removed using evacuation techniques.

CCDC 1447420, CCDC 1447421, CCDC 1447422 contain the supplementary crystallographic data for this paper. The data can be obtained free of charge from The Cambridge Crystallographic Data Centre via www.ccdc.cam.ac.uk/structures.

2.2.3. CO_2 Adsorption

CO_2 adsorption was performed using a Hiden Isochema Ltd. Intelligent Gravimetric Analyzer (Model IGA003, Warrington, UK) at 273 K. To minimize sample degradation from exposure to air, samples were added to the sample holder without drying to any degree, by removing the crystals from the mother liquor and transferring them directly to the holder. Wet sample masses were ~20 mg; application of a vacuum permitted drying at room temperature for a period of 72 h, ensuring all mother liquor was removed but sample integrity was retained via the mild degas conditions used. Dry masses, after this time, were ~16 mg. CO_2 uptakes of the dry samples were subsequently determined using adsorption-desorption cycles up to a maximum pressure of 1 MPa.

3. Results and Discussion

3.1. 1D Chain Coordination Polymer: [Zn(pytz(hydrolyzed))$_2$(OH$_2$)$_2$(OCOCH$_3$)$_2$]· H$_2$O

The formula unit for Zn-pytz(hydro) was resolved as triclinic with a space group of P-1 with total atoms: $ZnC_{26}H_{30}N_8O_{10}$ (Figure 1), giving an overall general formula of [Zn(pytz(hydrolyzed))$_2$(OH$_2$)$_2$(OCOCH$_3$)$_2$]· H$_2$O (molecular weight 679.95 g· mol^{-1} and volume 728.50 Å^3).

(**a**) (**b**)
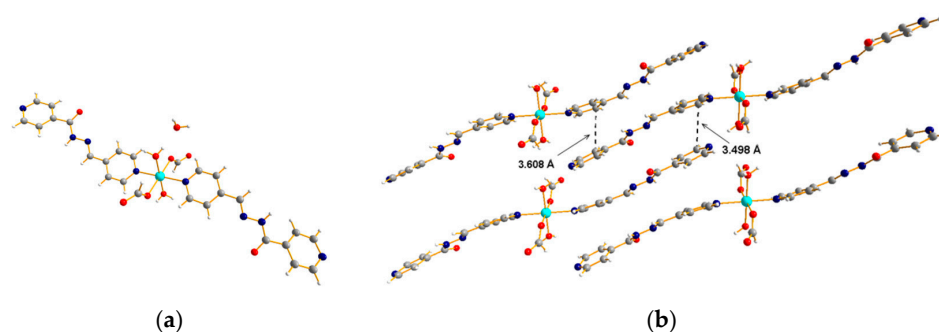
Figure 1. (**a**) Unit Structure of [Zn(pytz(hydrolyzed))$_2$(OH$_2$)$_2$(OCOCH$_3$)$_2$]· H$_2$O; (**b**) Possible π stacking interactions between 1D chains; Zn (**cyan**), C (**grey**), H (**white**), N (**blue**), O (**red**).

The structure resolved via SCXRD from this reaction can be seen in Figure 1a; it is clear that the pytz linker has been partially hydrolyzed with cleavage of the middle aromatic ring possibly as the result of the harsh conditions invoked by autoclave synthesis; these conditions also result in the decomposition of dimethylformamide to methanoic acid and diethylamine, which proton exchange to produce charged species. The negatively charged methanoic acid derivative reacts with

zinc centers to displace the coordinated nitrate anions. The overall structure formed is a 1D chain discreet coordination compound, Figure 1b highlights potential offset π-σ aromatic ring interactions occurring during packing and the distances marked (3.498–3.608 Å) are comparable with previously reported values [35]. Water solvent molecules were removed from the structure and void calculations (step size 0.4 Å) showed no pores accessible by CO_2, with the largest void sizes achieved (<0.7 Å) being too small for any guest species, even hydrogen. The proximity of the guest water molecules to the waters coordinated to Zn, the methanoic acids again coordinated to Zn and the carbonyl group of the ligand suggest that there are significant hydrogen bonding interactions, which may contribute to structure stability (see Supporting Information).

### 3.2. 1D Ladder Coordination Polymer: [Ni(pytz)$_{1.5}$(NO$_3$)]· nDCM (n = 2–3)

The formula unit for Ni-pytz was resolved as monoclinic with a space group of P2$_1$/c with total atoms: $NiC_{18.5}H_{13}ClN_{11}O_6$ (Figure 2), giving an overall general formula of $[Ni(pytz)_{1.5}(NO_3)_2] \cdot nDCM$, where n = 2–3 (molecular weight 579.56 g·mol^{-1} and volume 5534.4 Å^3).
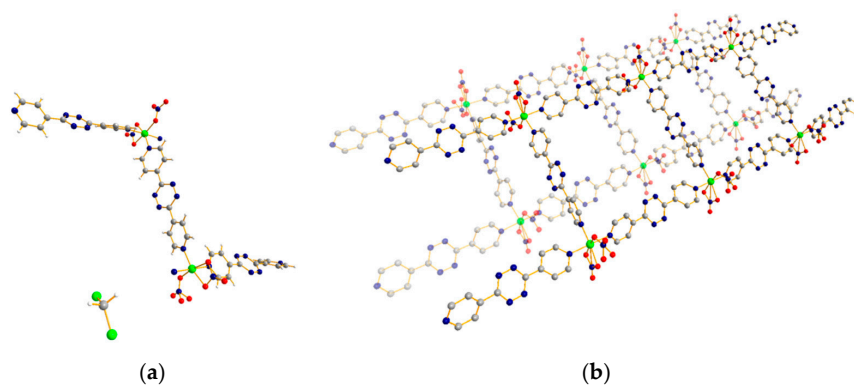
Figure 2. (**a**) Unit Structure of $[Ni(pytz)_{1.5}(NO_3)_2] \cdot nDCM$ (n = 2–3); (**b**) 1D ladder structure; Ni (**green**), C (**grey**), H (**white**), N (**blue**), O (**red**). DCM and ligand H atoms omitted for clarity in (**b**).

3.3. 1D Ladder Coordination Polymer: [Co$_2$(pytz)$_3$(NO$_3$)$_4$]· nDCM (n = 4–6)

The formula unit for Co-pytz was resolved as monoclinic with a space group of P2$_1$/c with total atoms: $Co_2C_{37}H_{26}Cl_2N_{22}O_{12}$ (Figure 3), giving an overall general formula of $[Co_2(pytz)_3(NO_3)_4] \cdot nDCM$, where n = 4–6 (molecular weight 1159.56 g·mol^{-1} and volume 5607.9 Å^3). Co-pytz is isostructural to Ni-pytz; Co-pytz is used to demonstrate the unit structure and overall ladder structure obtained (Figure 3).
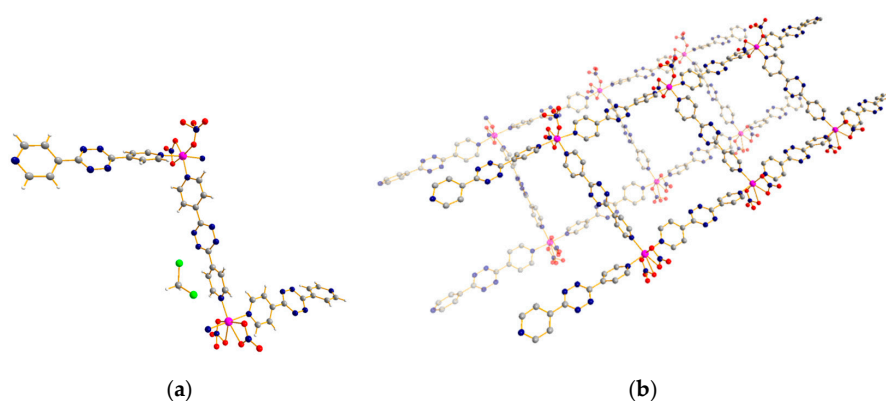

Figure 3. (**a**) Unit Structure of $[Co_2(pytz)_3(NO_3)_4] \cdot nDCM$ (n = 4–6); (**b**) 1D ladder structure; Co (**magenta**), C (**grey**), H (**white**), N (**blue**), O (**red**). DCM and ligand H atoms omitted for clarity in (**b**).

The 1D ladders pack to form a 3D network with 14 × 7.4 Å pores between the chains, the dimensions, as shown in Figure 4. Each Co/Ni is bonded to two nitrate groups: one ordered and one disordered and it is suggested that the structure is held together by face-edge-face π-stacking of the component aromatic rings; ~3.4–3.6 Å in length, these electrostatic interactions are shorter than typical π stacking distances (4.3–4.9 Å [36]), indicating slightly stronger interactions, which contribute to structural integrity. These π stacking interactions are significantly affected by the positioning and rotation of the pytz linker within the structure; in some crystallographic domains, only T-shaped stacking can occur, where one side of the tetrazine is in close proximity with the pyridyl ring. DCM solvent molecules within the pores also contribute to the structural integrity of the material. Only one well ordered DCM molecule was retained in the model structure; the placement and distance (2.77 Å) suggests this DCM is hydrogen bonded to the nitrate group bonded to the Co/Ni. Further disordered DCM molecules were present in the pores but were removed from the model using SQUEEZE. The orientation of subsequent solvent molecules indicates they would also exhibit hydrogen bonds with neighboring nitrate groups within the structure. Void calculations (grid step size 0.4 Å, grid point radius 1.76 Å) indicated that the porosity extends beyond one unit cell, into the interconnected structure, suggesting ease of diffusion for suitably sized guest species throughout the whole structure; this regular porosity is produced by the layering of multiple offset ladders (Figure 5). Smaller pores also exist between voids, but are too small to allow transport of gas molecules through the structure, thus are inaccessible in terms of gas adsorption.
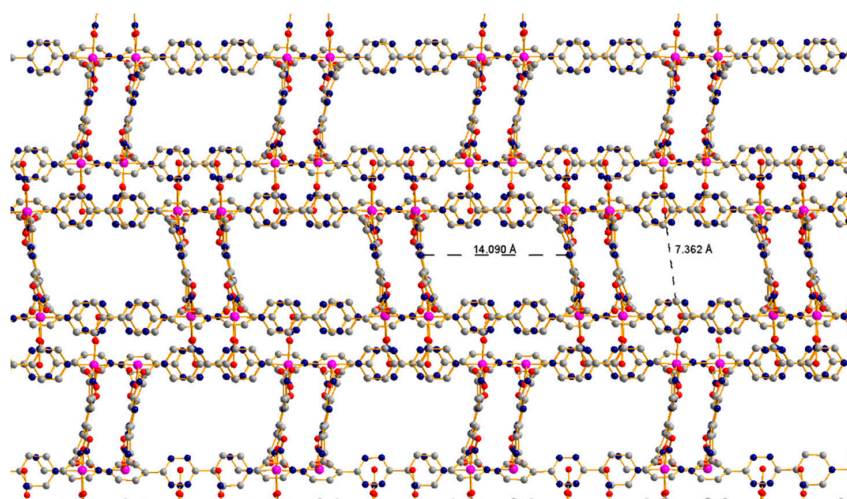
Figure 4. Co-pytz (isostructural to Ni(pytz)) view along a-axis; pore window sizes determined for DCM inclusion. DCM and ligand H atoms omitted from image for clarity. Co (**purple**), C (**grey**), N (**blue**), O (**red**).
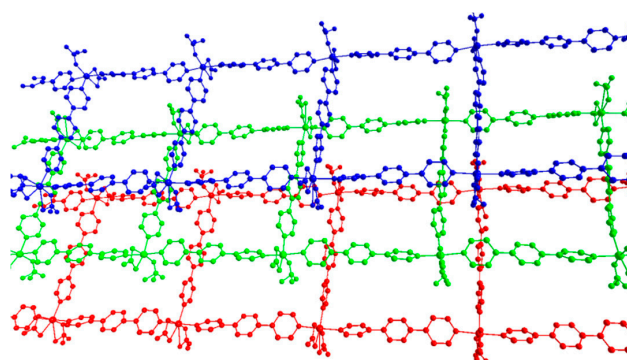
Figure 5. Co-pytz offset layered ladders demonstrating interconnected porosity; front ladder—blue, second—red, third—green. DCM and ligand H atoms omitted from image for clarity.

The porous structure of the isostructural Co-pytz and Ni-pytz suggested these materials may be suitable for gas storage applications and Co-pytz was characterized using CO_2 adsorption.

3.4. CO_2 Adsorption of Co-pytz

Isothermal adsorption of CO_2 at 273 K up to 1 MPa (Figure 6), produced a Type I isotherm with a small degree of hysteresis; all points equilibrated within a maximum time of 40 min, suggesting excellent kinetic performance of the materials for the probe gas. The maximum CO_2 uptake on Co-pytz, at 273 K, was 1.08 mmol·g^{-1} at 1 MPa (p/p_0 = 0.28); which, considering the uncoordinated nitrogen functionalities available within the structure for CO_2 adsorption, equates to a loading of 15 wt %. This uptake is comparable with existing systems and the system demonstrates favorable charging times, which are essential for industrial application of these materials.
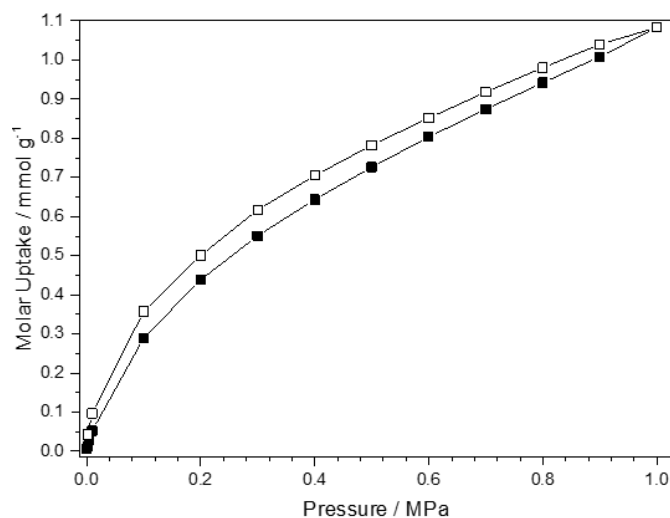

Figure 6. Sorption isotherm for CO_2 on Co-pytz at 273 K.

4. Conclusions

Three MOF structures were synthesized using transition metal based Secondary Building Units (SBUs) and the pytz linker, all are 1D structure, Zn producing a chain structure, while Ni and Co create ladder MOFs. Increased dimensionality of a MOF is assumed to enhance the adsorption potential, and these 1D materials would be expected to show low uptakes, however, CO_2 adsorption measurements on Co-pytz at 273 K show a reasonable uptake, which could have potential for carbon capture applications. The maximum uptake was 1.08 mmol or 47.5308 mg CO_2/g Co-pytz (at 1 MPa), equating to 15 wt % based on the available nitrogen within the structure. These early results suggest that, if the dimensionality of pytz based MOF materials could be increased, from 1D, it may be possible to increase available porosities, hence, CO_2 capacities.

Author Contributions: Edmund J. Cussen and Ashleigh J. Fletcher conceived and designed the experiments; Emma Dooris, Craig A. McAnally and Alan R. Kennedy performed the experiments and analyzed the data; Edmund J. Cussen, Ashleigh J. Fletcher and Alan R. Kennedy contributed reagents/materials/analysis tools; Ashleigh J. Fletcher wrote the paper.

Conflicts of Interest: The authors declare no conflict of interest.

References

1. Furukawa, H.; Cordova, K.E.; O'Keeffe, M.; Yaghi, O.M. The chemistry and applications of metal-organic frameworks. *Science* **2013**, *341*, 1230444. [CrossRef] [PubMed]
2. He, Y.; Zhou, W.; Qian, G.; Chen, B. Methane storage in metal-organic frameworks. *Chem. Soc. Rev.* **2014**, *43*, 5657–5678. [CrossRef] [PubMed]
3. Sumida, K.; Rogow, D.L.; Mason, J.A.; McDonald, T.M.; Bloch, E.D.; Herm, Z.R.; Bae, T.-H.; Long, J.R. Carbon dioxide capture in metal-organic frameworks. *Chem. Rev.* **2011**, *112*, 724–781. [CrossRef] [PubMed]
4. Lee, J.; Farha, O.K.; Roberts, J.; Scheidt, K.A.; Nguyen, S.T.; Hupp, J.T. Metal-organic framework materials as catalysts. *Chem. Soc. Rev.* **2009**, *38*, 1450–1459. [CrossRef] [PubMed]
5. Liu, J.; Chen, L.; Cui, H.; Zhang, J.; Zhang, L.; Su, C.-Y. Applications of metal-organic frameworks in heterogeneous supramolecular catalysis. *Chem. Soc. Rev.* **2014**, *43*, 6011–6061. [CrossRef] [PubMed]
6. Hu, Z.; Deibert, B.J.; Li, J. Luminescent metal-organic frameworks for chemical sensing and explosive detection. *Chem. Soc. Rev.* **2014**, *43*, 5815–5840. [CrossRef] [PubMed]
7. Kreno, L.E.; Leong, K.; Farha, O.K.; Allendorf, M.; van Duyne, R.P.; Hupp, J.T. Metal-organic framework materials as chemical sensors. *Chem. Rev.* **2011**, *112*, 1105–1125. [CrossRef] [PubMed]
8. Cui, Y.; Chen, B.; Qian, G. Lanthanide metal-organic frameworks for luminescent sensing and light-emitting applications. *Coord. Chem. Rev.* **2014**, *273*, 76–86. [CrossRef]
9. Li, J.-R.; Ma, Y.; McCarthy, M.C.; Sculley, J.; Yu, J.; Jeong, H.-K.; Balbuena, P.B.; Zhou, H.-C. Carbon dioxide capture-related gas adsorption and separation in metal-organic frameworks. *Coord. Chem. Rev.* **2011**, *255*, 1791–1823. [CrossRef]
10. Suh, M.P.; Park, H.J.; Prasad, T.K.; Lim, D.-W. Hydrogen storage in metal-organic frameworks. *Chem. Rev.* **2011**, *112*, 782–835. [CrossRef] [PubMed]
11. Li, J.-R.; Sculley, J.; Zhou, H.-C. Metal-organic frameworks for separations. *Chem. Rev.* **2011**, *112*, 869–932. [CrossRef] [PubMed]
12. Qiu, S.; Xue, M.; Zhu, G. Metal-organic framework membranes: From synthesis to separation application. *Chem. Soc. Rev.* **2014**, *43*, 6116–6140. [CrossRef] [PubMed]
13. Intergovenmental Panel on Climate Change. *Intergovernmental Panel on Climate Change (IPCC) Fifth Assessment Report: Climate Change*; Intergovenmental Panel on Climate Change: Genève, Switzerland, 2014.
14. Rochelle, G.T. Amine scrubbing for CO_2 capture. *Science* **2009**, *325*, 1652–1654. [CrossRef] [PubMed]
15. Kuppler, R.J.; Timmons, D.J.; Fang, Q.-R.; Li, J.-R.; Makal, T.A.; Young, M.D.; Yuan, D.; Zhao, D.; Zhuang, W.; Zhou, H.-C. Potential applications of metal-organic frameworks. *Coord. Chem. Rev.* **2009**, *253*, 3042–3066. [CrossRef]
16. Shekhah, O.; Liu, J.; Fischer, R.; Wöll, C. MOF thin films: Existing and future applications. *Chem. Soc. Rev.* **2011**, *40*, 1081–1106. [CrossRef] [PubMed]
17. Li, J.-R.; Kuppler, R.J.; Zhou, H.-C. Selective gas adsorption and separation in metal-organic frameworks. *Chem. Soc. Rev.* **2009**, *38*, 1477–1504. [CrossRef] [PubMed]
18. Shah, M.; McCarthy, M.C.; Sachdeva, S.; Lee, A.K.; Jeong, H.-K. Current status of metal-organic framework membranes for gas separations: Promises and challenges. *Ind. Eng. Chem. Res.* **2012**, *51*, 2179–2199. [CrossRef]
19. Eddaoudi, M.; Li, H.L.; Yaghi, O.M. Highly porous and stable metal-organic frameworks: Structure design and sorption properties. *J. Am. Chem. Soc.* **2000**, *122*, 1391–1397. [CrossRef]
20. Ferey, G. Hybrid porous solids: Past, present, future. *Chem. Soc. Rev.* **2008**, *37*, 191–214. [CrossRef] [PubMed]
21. Kitagawa, S.; Kitaura, R.; Noro, S. Functional porous coordination polymers. *Angew. Chem. Int. Ed.* **2004**, *43*, 2334–2375. [CrossRef] [PubMed]
22. Nugent, P.; Belmabkhout, Y.; Burd, S.D.; Cairns, A.J.; Luebke, R.; Forrest, K.; Pham, T.; Ma, S.; Space, B.; Wojtas, L. Porous materials with optimal adsorption thermodynamics and kinetics for CO_2 separation. *Nature* **2013**, *495*, 80–84. [CrossRef] [PubMed]
23. Zhang, Z.; Zhao, Y.; Gong, Q.; Li, Z.; Li, J. MOFs for CO_2 capture and separation from flue gas mixtures: The effect of multifunctional sites on their adsorption capacity and selectivity. *Chem. Commun.* **2013**, *49*, 653–661. [CrossRef] [PubMed]
24. Chen, B.; Xiang, S.; Qian, G. Metal-organic frameworks with functional pores for recognition of small molecules. *Acc. Chem. Res.* **2010**, *43*, 1115–1124. [CrossRef] [PubMed]
25. Caskey, S.R.; Wong-Foy, A.G.; Matzger, A.J. Dramatic tuning of carbon dioxide uptake via metal substitution in a coordination polymer with cylindrical pores. *J. Am. Chem. Soc.* **2008**, *130*, 10870–10871. [CrossRef] [PubMed]

26. Couck, S.; Denayer, J.F.; Baron, G.V.; Rémy, T.; Gascon, J.; Kapteijn, F. An amine-functionalized MIL-53 metal-organic framework with large separation power for CO_2 and CH_4. *J. Am. Chem. Soc.* **2009**, *131*, 6326–6327. [CrossRef] [PubMed]

27. Vaidhyanathan, R.; Iremonger, S.S.; Shimizu, G.K.; Boyd, P.G.; Alavi, S.; Woo, T.K. Direct observation and quantification of CO_2 binding within an amine-functionalized nanoporous solid. *Science* **2010**, *330*, 650–653. [CrossRef] [PubMed]

28. Li, B.; Zhang, Z.; Li, Y.; Yao, K.; Zhu, Y.; Deng, Z.; Yang, F.; Zhou, X.; Li, G.; Wu, H. Enhanced binding affinity, remarkable selectivity, and high capacity of CO_2 by dual functionalization of a rht-type metal-organic framework. *Angew. Chem. Int. Ed.* **2012**, *51*, 1412–1415. [CrossRef] [PubMed]

29. Millward, A.R.; Yaghi, O.M. Metal-organic frameworks with exceptionally high capacity for storage of carbon dioxide at room temperature. *J. Am. Chem. Soc.* **2005**, *127*, 17998–17999. [CrossRef] [PubMed]

30. Bisht, K.K.; Suresh, E. Spontaneous resolution to absolute chiral induction: Pseudo-kagomé type homochiral Zn(II)/Co(II) coordination polymers with achiral precursors. *J. Am. Chem. Soc.* **2013**, *135*, 15690–15693. [CrossRef] [PubMed]

31. Hijikata, Y.; Horike, S.; Sugimoto, M.; Inukai, M.; Fukushima, T.; Kitagawa, S. Pore design of two-dimensional coordination polymers toward selective adsorption. *Inorg. Chem.* **2013**, *52*, 3634–3642. [CrossRef] [PubMed]

32. Hulvey, Z.; Furman, J.D.; Turner, S.A.; Tang, M.; Cheetham, A.K. Dimensionality trends in metal-organic frameworks containing perfluorinated or nonfluorinated benzenedicarboxylates. *Cryst. Growth Des.* **2010**, *10*, 2041–2043. [CrossRef]

33. Sheldrick, G.M. A short history of shelx. *Acta Crystallogr. Sect. A Found. Crystallogr.* **2007**, *64*, 112–122. [CrossRef] [PubMed]

34. Greenwood, N.N.; Earnshaw, A. *Chemistry of the Elements*; Butterworth Heinemann: Oxford, UK, 1998.

35. Hunter, C.A.; Sanders, J.K. The nature of π-π. Interactions. *J. Am. Chem. Soc.* **1990**, *112*, 5525–5534. [CrossRef]

36. Felloni, M.; Blake, A.J.; Hubberstey, P.; Wilson, C.; Schroder, M. Hydrogen-bonding interactions between linear bipyridinium cations and nitrate anions. *CrystEngComm* **2002**, *4*, 483–495. [CrossRef]